The Journal of Experimental Biology 216, 601-613

doi:10.1242/jeb.077164

RESEARCH ARTICLE

Cardioacceleratory function of the neurohormone CCAP in the mosquito *Anopheles gambiae*

Tania Y. Estévez-Lao, Dacia S. Boyce, Hans-Willi Honegger and Julián F. Hillyer*

Department of Biological Sciences, Vanderbilt University, Nashville, TN 37235, USA

*Author for correspondence (julian.hillyer@vanderbilt.edu)

SUMMARY

Crustacean cardioactive peptide (CCAP) is a highly conserved arthropod neurohormone that is involved in ecdysis, hormone release and the modulation of muscle contractions. Here, we determined the CCAP gene structure in the malaria mosquito *Anopheles gambiae*, assessed the developmental expression of *CCAP* and its receptor and determined the role that CCAP plays in regulating mosquito cardiac function. RACE sequencing revealed that the *A. gambiae CCAP* gene encodes a neuropeptide that shares 100% amino acid identity with all sequenced CCAP peptides, with the exception of *Daphnia pulex*. Quantitative RT-PCR showed that expression of *CCAP* and the CCAP receptor displays a bimodal distribution, with peak mRNA levels in second instar larvae and pupae. Injection of CCAP revealed that augmenting hemocoelic CCAP levels in adult mosquitoes increases the anterograde and retrograde heart contraction rates by up to 28%, and increases intracardiac hemolymph flow velocities by up to 33%. Partial *CCAP* knockdown by RNAi had the opposite effect, decreasing the mosquito heart rate by 6%. Quantitative RT-PCR experiments showed that *CCAP* mRNA is enriched in the head region, and immunohistochemical experiments in newly eclosed mosquitoes detected CCAP in abdominal neurons and projections, some of which innervated the heart, but failed to detect CCAP in the abdomens of older mosquitoes. Instead, in older mosquitoes CCAP was detected in the pars lateralis, the subesophageal ganglion and the corpora cardiaca. In conclusion, CCAP has a potent effect on mosquito circulatory physiology, and thus heart physiology in this dipteran insect is under partial neuronal control.

Supplementary material available online at http://jeb.biologists.org/cgi/content/full/216/4/601/DC1

Key words: dorsal vessel, heart, hemolymph, crustacean cardioactive peptide, neuropeptide, circulatory system, insect, Diptera, Culicidae.

Received 9 July 2012; Accepted 23 October 2012

INTRODUCTION

The insect circulatory system functions in nutrient transport, waste removal, hormone delivery, immune surveillance, thermoregulation and respiration (Wasserthal, 2003; Klowden, 2007; Babcock et al., 2008; Nation, 2008; Wasserthal, 2012). Anatomically, the insect circulatory system is composed of hemolymph (blood), an open body cavity called the hemocoel, and a series of pumps (Klowden, 2007; Nation, 2008). The primary pump is called the dorsal vessel, which is a muscular tube that extends the length of the body and is subdivided into an abdominal heart and a thoracic aorta. In mosquitoes, the heart propels hemolymph toward the head (anterograde) and the posterior of the abdomen (retrograde) by periodically alternating the direction in which wave-like contractions propagate (Andereck et al., 2010; Glenn et al., 2010). When the heart contracts anterograde, hemolymph enters the vessel's lumen through paired valves, called ostia, that are located in the anterior portion of each abdominal segment, and exits the vessel through an excurrent opening located near the posterior of the head. When the heart contracts retrograde, hemolymph enters the vessel through a single pair of ostia located at the thoraco-abdominal junction and exits through a pair of excurrent openings located in the last abdominal segment (Glenn et al., 2010).

Although the mosquito heart is essential for basic physiological processes (Klowden, 2007; Nation, 2008), and may also influence the ability of pathogens such as malaria to be transmitted (Hillyer et al., 2007), little is known about the factors that regulate heart contraction rates and contraction direction. In other insects, the heart contracts in a myogenic manner (Jones, 1977; Dulcis et al., 2001; Sláma and Lukáš, 2011), but several neurohormones and neurotransmitters affect the speed and directionality of heart contractions (Johnson et al., 1997; Dulcis and Levine, 2005; Dulcis et al., 2005; Nichols, 2006; Lee et al., 2012; Setzu et al., 2012). Among the cardiostimulatory neurohormones is crustacean cardioactive peptide (CCAP), a cyclic amidated nonapeptide that is produced in a broad range of organisms, including crabs (Stangier et al., 1987), crayfish (Chung et al., 2006), lobsters (Chung et al., 2006), ticks (Simo et al., 2009), mites (Christie et al., 2011) and all sequenced insect lineages (Cheung et al., 1992; Furuya et al., 1993; Riehle et al., 2002; Park et al., 2003; Sakai et al., 2004; Predel et al., 2010; Lee et al., 2011), which suggests that CCAP was produced by the ancestral arthropod. CCAP was originally isolated from the pericardial organs of the shore crab, *Carcinus maenas*, because of its cardioacceleratory effect on semi-isolated crab heart preparations (Stangier et al., 1987). In insects, CCAP is a pleiotropic peptide that functions in diverse processes such as ecdysis (Ewer and Reynolds, 2002; Arakane et al., 2008; Lahr et al., 2012), hormone release (Veelaert et al., 1997), contraction of the gut and oviduct (Donini et al., 2001; Sakai et al., 2004) and the regulation of various cardiac parameters (Furuya et al., 1993; Lehman et al., 1993; Dulcis et al., 2005; Wasielewski and Skonieczna, 2008; da Silva et al., 2011).

In mosquitoes, the function of CCAP remains unknown, but two reports suggest that a bioactive CCAP peptide–receptor combination

Table 1. Sequences of primers used in this study

Gene	Vectorbase ID		Nucleotide sequence (5′–3′)	Amplicon (bp) Transcript	Amplicon (bp) Genomic	Application
CCAP	AGAP009729	Forward	GCTGGCAGTTGTATCGCTCT	406	480	PCR-S
		Reverse	GCCCGACTTTTGCAGATAAA			
CCAP	AGAP009729	Forward	GCTGGCAGTTGTATCGCTCT	127	201	qPCR
		Reverse	GGTAAAGGCGTTGCAGAAC			
CCAP	AGAP009729	Forward	TAATACGACTCACTATAGGACCCAGGGCGGAAGG	192[a]	192[a]	RNAi
		Reverse	TAATACGACTCACTATAGGTTCGCTTCCTGGATCG			
		Forward	TAATACGACTCACTATAGGGCCTACAAACAGTACAACAC	669[a]	669[a]	RNAi
		Reverse	TAATACGACTCACTATAGGGAAGCCGTGTATTGATTA			
CCAP	AGAP009729	Reverse	CGCAACCGGTAAAGGCGTTGCAGAAC	n.a.	n.a.	5' RACE
CCAP	AGAP009729	Forward	GGCCAAGCTGCTGCTGGCAGTTGTATC	n.a.	n.a.	3' RACE
CCAP	AGAP009729	Forward	GGCGGAAGGACCGTATGGGCAGTGATT	n.a.	n.a.	3' RACE n
CCAPR	AGAP001962	Forward	GTAAAGCAATCCGCTTCGTC	806	1818	PCR-S
		Reverse	ACTGCTGTTGTGGTTGTGGA			
CCAPR	AGAP001962	Forward	GTAAAGCAATCCGCTTCGTC	180	254	qPCR
		Reverse	TCGGCAGGGAGAAAAGTATG			
CCAPR	AGAP001962	Forward	TAATACGACTCACTATAGGTATGGCAGATCTGGCGAC	302[a]	302[a]	RNAi
		Reverse	TAATACGACTCACTATAGGCACACCTGCGTGGAGAA			
RPS7	AGAP010592	Forward	GACGGATCCCAGCTGATAAA	132	281	qPCR
		Reverse	GTTCTCTGGGAATTCGAACG			
RSPS17	AGAP004887	Forward	GACGAAACCACTGCGTAACA	153	264	qPCR
		Reverse	TGCTCCAGTGCTGAAACATC			
bla(Ap^R)	(Bacterial gene)	Forward	TAATACGACTCACTATAGGGCCGAGCGCAGAAGTGGT	214[a]	214[a]	RNAi
		Reverse	TAATACGACTCACTATAGGGAACCGGAGCTGAATGAA			

Vectorbase IDs were obtained from the AgamP3 assembly in www.vectorbase.org [exception: *bla(Ap^R)*].
Underlined sequences are specific to the T7 RNA polymerase promoter sites needed for dsRNA synthesis.
Primers were used for the following applications: PCR-S, sequencing; qPCR, quantitative PCR; RNAi, synthesis of dsRNA; 5′ RACE/3′ RACE, sequencing of terminal ends; 3′ RACE n, nested primer for 3′ RACE.
[a]RNAi amplicon lengths include the T7 promoter sequence tags.
n.a., not applicable. The other primer in these pairs was a GeneRacer RACE primer (Invitrogen).

is present in the culicid lineage. First, using a heterologous expression system, Belmont et al. (Belmont et al., 2006) showed that the then putative *Anopheles gambiae* CCAP receptor has strong affinity for the CCAP peptide. Then, Honegger et al. (Honegger et al., 2011) showed that specific neurons in the mosquito ventral nerve cord produce both CCAP and bursicon, and that these neurons undergo apoptosis several hours after adult ecdysis. Here, we describe the structure of the *CCAP* gene in the malaria mosquito *A. gambiae*, assess *CCAP* expression during development, and show that in adult mosquitoes CCAP has potent cardioacceleratory activity.

MATERIALS AND METHODS

Mosquito rearing and maintenance

Anopheles gambiae Giles *sensu stricto* (G3 strain; Diptera: Culicidae) eggs were hatched in distilled water and larvae were fed a combination of koi food and yeast. Upon pupation, mosquitoes were transferred to 4.7 l plastic containers with a marquisette top, and adults were fed a 10% sucrose solution *ad libitum*. All mosquito stages were maintained in an environmental chamber at 27°C and 75% relative humidity, under a 12 h:12 h light:dark cycle that included 30 min crepuscular periods. Unless otherwise stated, all experiments were carried out on 5-day-old adult females.

cDNA synthesis, PCR, sequencing and rapid amplification of cDNA ends

RNA from 10–20 mosquitoes was isolated using TRIzol Reagent (Invitrogen, Carlsbad, CA, USA), re-purified using the RNeasy Mini Kit (Qiagen, Valencia, CA, USA) and treated with RQ1 RNase-free DNase (Promega, Madison, WI, USA). Up to 5 μg of RNA was then used for cDNA synthesis using an Oligo(dt)$_{20}$ primer and the SuperScript III First-Strand Synthesis System for RT-PCR (Invitrogen). Each cDNA preparation was then treated with RNase H.

To begin sequencing *CCAP*, the central region of *A. gambiae CCAP* was amplified using gene-specific primers and high fidelity/high specificity Accuprime Pfx SuperMix (Invitrogen) on a DNA Engine Thermal Cycler (Bio-Rad, Hercules, CA, USA). Amplicons were purified using the PureLink PCR Purification Kit (Invitrogen), cloned using Invitrogen's TOPO TA Cloning Kit for Sequencing, and plasmids were isolated using Qiagen's Plasmid Mini Kit. Inserts were then sequenced using BigDye Terminator v3.1 chemistry and a vector-specific primer on a 3730xl DNA Analyzer (Applied Biosystems, Foster City, CA, USA) managed by Vanderbilt University's DNA sequencing facility. The resulting trace files were analyzed using 4Peaks software (Mek and Tosj, Amsterdam, The Netherlands).

The 5′ and 3′ terminal ends of *CCAP* were sequenced by rapid amplification of cDNA ends (RACE). To sequence the 5′ terminal region, a 5′/3′ RACE library was constructed using Invitrogen's GeneRacer kit, and the 5′ end of *CCAP* was amplified by PCR using a gene-specific primer and a GeneRacer primer. The resulting mixture was separated by agarose gel ectrophoresis, the band was excised using Qiagen's QIAquick Gel Extraction kit, and the purified amplicons were cloned, sequenced and analyzed as described above. The same protocol was followed to sequence the 3′ terminal region except that a nested PCR was performed prior to cloning. For a list of primers used in this study see Table 1.

Nucleotide sequences were aligned using the BL2SEQ tool in the National Center for Biotechnology Information (http://blast.ncbi.nlm.nih.gov/), and after assembly, sequences were graphically visualized using Artemis software (Wellcome Trust Sanger Institute, Cambridge, UK). The predicted CCAP protein mass was calculated using the Compute pI/Mw tool in the ExPASy Bioinformatics Resource Portal (http://web.expasy.org/compute_pi/), and the location of the signal peptide was predicted using the SignalP 4.0 server (Petersen et al., 2011). Finally, alignment of CCAP proteins encoded by members of the order Diptera was carried out using ClustalW2 (http://www.ebi.ac.uk/Tools/msa/clustalw2/).

Gene expression analyses

CCAP and CCAP receptor (*CCAPR*) gene expression was quantified as described for *CRZ* (Hillyer et al., 2012). To quantify the developmental expression of *CCAP* and *CCAPR*, cDNA was constructed from RNA purified from ~200 eggs, 50 second instar larvae, 40 third instar larvae, 30 fourth instar larvae, 20 pupae (callow or black) or 15 adults (24 h, 5 days or 10 days old). Transcript levels of *CCAP* and *CCAPR* were measured by real-time quantitative PCR (qPCR) using SYBR Green PCR Master Mix (Applied Biosystems) on an ABI 7300 Real-Time PCR system. *RPS7* was used as the loading reference (Coggins et al., 2012), and relative quantification of *CCAP* and *CCAPR* mRNA levels was performed using the $2^{-\Delta\Delta C_T}$ method (Livak and Schmittgen, 2001). Three biological replicates were conducted and each was analyzed in duplicate. The graphed output displays the average fold-change in mRNA levels relative to eggs. Finally, transcription of *RPS17* was measured to validate the *RPS7* reference. Transcriptional patterns of *RPS7* and *RPS17* were similar, and analysis of the *CCAP* and *CCAPR* data using either housekeeping gene as the reference yielded similar results.

To quantify *CCAP* expression in different body segments, cDNA was synthesized from RNA purified from 10 whole bodies, 20 heads, 20 thoraces or 20 abdomens from adult mosquitoes at <1 h or 5 days post-eclosion. Transcript levels were analyzed as above, with the graphed output displaying the average mRNA fold-difference relative to 5-day-old whole bodies. All primer pairs used in these experiments amplify fragments that span an intron (Table 1), and melting curve analyses were performed at the end of each qPCR run to confirm that the cDNA preparations lacked genomic DNA. Data were statistically analyzed by ANOVA (developmental expression) or two-way ANOVA (body segment expression at different ages). Differences were deemed significant at $P<0.05$.

Measurement of heart contraction dynamics: CCAP injection

CCAP peptide, sequence H-PFCNAFTGC-NH2 (including a disulfide bond between the cysteines), was purchased from Bachem Americas (Torrance, CA, USA). Stock solutions were prepared as described previously (da Silva et al., 2011). For physiological manipulations, mosquitoes were cold anesthetized and restrained dorsal side up on Sylgard 184 silicone elastomer plates (Dow Corning, Midland, MI, USA) using a non-invasive method previously described and pictured (Andereck et al., 2010). After mosquitoes acclimated to room temperature, 60 s videos of their dorsal abdomen were recorded under brightfield trans illumination using a Nikon SMZ1500 stereo microscope (Nikon, Tokyo, Japan) connected to a Photometrics CoolSNAP HQ2 high sensitivity monochrome CCD camera (Roper Scientific, Ottobrunn, Germany) and Nikon Advanced Research NIS-Elements software. Each mosquito was then injected through the thoracic anepisternal cleft with ~0.2 µl of phosphate buffered saline (pH 7.0; PBS) or various concentrations of synthetically produced CCAP in PBS (1×10^{-3} to 1×10^{-10} mol l^{-1}, which is diluted ~1:5 as it mixes with the hemolymph). After allowing the injected solution to circulate with the hemolymph for 10 min, a second 60 s recording was acquired, thus yielding for each mosquito paired videos that recorded both basal heart physiology and heart physiology following treatment (PBS or various concentrations of CCAP). Each video was acquired at 25.6 frames s^{-1} (27 ms exposures, 3×3 binning and 1× calibrated gain) and manually analyzed using NIS-Elements software. By visualizing the direction and frequency of wave-like contractions of the heart throughout the length of the abdomen, the following parameters were measured: (1) total contraction rate (Hz; contractions s^{-1}), (2) anterograde contraction rate (while the heart contracts toward the head), (3) retrograde contraction rate (while the heart contracts toward the posterior abdomen), (4) heartbeat directional reversals (times per minute that the heart reverses from contracting anterograde to contracting retrograde and vice versa), (5) percentage of contractions propagating in the anterograde direction, (6) percentage of contractions propagating in the retrograde direction, (7) percentage of time the heart contracts in the anterograde direction and (8) percentage of time the heart contracts in the retrograde direction. Finally, as an observer control, a subset of the videos was re-analyzed blindly by a second researcher, and comparison of the readings confirmed the objectivity of the data. For videos of contracting hearts imaged using this methodology, see Movie 1 in the supplementary material and our previously published work (Andereck et al., 2010; Glenn et al., 2010; Hillyer et al., 2012).

The paired data were statistically analyzed using repeated measures two-way ANOVA, with the *P*-value relevant to this study assessing whether there is a significant dose-dependent effect of CCAP injection on heart physiology (interaction). Sidak's *post hoc* tests then compared the pre- and post-injection values for each individual CCAP dose or PBS treatment. For the parameters where there was a dose-dependent effect of CCAP treatment on heart physiology (interaction), the ratios of post- and pre-treatment were calculated and the resultant values were statistically analyzed using the Kruskal–Wallis test. *Post hoc* multiple comparisons were carried out using Dunn's test. Differences were deemed significant at $P<0.05$.

Measurement of hemolymph flow velocity

Cold-anesthetized and restrained mosquitoes were allowed to stabilize to room temperature and were injected through the anepisternal cleft with ~0.2 µl of either PBS or 1×10^{-7} mol l^{-1} CCAP in PBS. After allowing the injected solution to flow with the hemolymph for 10 min, mosquitoes were injected with ~0.1 µl of a 1:1500 dilution of 2 µm red fluorescent Fluosphere microspheres (Invitrogen). Immediately following the second injection, mosquitoes were video recorded for 60 s using low-level fluorescence illumination on the SMZ1500 microscope ensemble described above. Videos were acquired for each mosquito at 23.5 frames s^{-1}, using 40 ms exposures, 3×3 binning and a 4× calibrated gain. The manual feature of the Object Tracker module of NIS-Elements was then used to quantitatively track the trajectory of neutral density microspheres as they flowed through the heart, and these measurements were used to calculate the velocity of hemolymph flow by dividing the path length by the amount of time each particle was tracked. A total of 14 mosquitoes were analyzed, and for each mosquito 10 particles were tracked as they moved in the anterograde direction and five particles were tracked as they moved in the retrograde direction. All tracked particles traveled a

minimum distance of 625 μm, with mean tracking distances of 1528 and 1247 μm in the anterograde and retrograde directions, respectively. For statistical analyses, aggregated data were first separated by tracking direction (anterograde and retrograde), and then separated into the two treatment groups (PBS and CCAP). For each tracking direction, data were analyzed using the Mann–Whitney test. Differences were deemed significant at $P<0.05$.

Measurement of heart contraction dynamics: CCAP knockdown by RNA interference

In preparation for RNA interference (RNAi) experiments, cDNA fragments of target genes were amplified by PCR using gene-specific primers with T7 promoter tags. Amplicons were separated by agarose gel electrophoresis, the bands were excised and purified as above, and the purified amplicons were used as template in a second PCR reaction. The resulting amplicons were then purified using the PureLink PCR Purification Kit, and 1 μg of each product was used for double-stranded RNA (dsRNA) synthesis using the MEGAscript T7 Kit (Applied Biosystems). The resultant dsRNAs were ethanol precipitated and resuspended in RNase-free water, and their concentrations were quantified by measuring absorbance at an optical density of 260 nm (OD_{260}). The integrity of each dsRNA construct was determined by separating a small amount by agarose gel electrophoresis and estimating the size and concentration against New England Biolab's 100 bp DNA ladder (New England Biolabs, Ipswich, MA, USA). A total of three mosquito-specific dsRNA constructs were synthesized: 192 bp *CCAP*, 669 bp *CCAP* and 302 bp *CCAPR*. As a control, a 214 bp dsRNA construct specific to *bla*(Ap^R), the ampicillin-resistant gene that is encoded in Novagen's pET-46 Ek/LIC vector (EMD Chemicals, Gibbstown, NJ), was also synthesized from DNA purified from BL21(DE3) *Escherichia coli* cells containing the pET-46 plasmid.

To knockdown gene expression, 200–400 ng of dsRNA was injected into 1-day-old mosquitoes. Four days after dsRNA injection, mosquitoes were restrained and their heart physiology was measured as above. To verify knockdown efficiencies, immediately following video acquisition the whole bodies of mosquitoes were triturated in TRIzol, their homogenates were pooled, cDNA was synthesized and relative gene expression was quantified by qPCR as described for the developmental expression experiments. The calculated knockdown efficiencies for each treatment group represent the percent reduction in mRNA levels relative to the *bla*(Ap^R) dsRNA control group of each independent trial. This experimental design allowed for the measurement of heart physiology and gene knockdown in series, and thus the observed knockdown efficiencies are an exact representation of the transcriptional state of the mosquitoes physiologically assayed.

Five RNAi trials were conducted in this study: two silenced *CCAP* using the 192 bp dsRNA construct (N=18; knockdown efficiency average=47%), two silenced *CCAP* using the 669 bp dsRNA construct (N=27; knockdown efficiency average=54%), and one was a double knockdown experiment that silenced *CCAP* using the 669 bp dsRNA construct and *CCAPR* using the 302 bp dsRNA construct (N=15; knockdown efficiency=83 and 61%, respectively). Because the results in all trials exhibited an identical trend, the data were aggregated and analyzed using an unpaired two-tailed *t*-test. Differences were deemed significant at $P<0.05$.

CCAP immunohistochemistry

Whole-mount immunolabeling in the mosquito abdomen was carried out as described previously (Honegger et al., 2011), except that both the dorsal and ventral halves were analyzed. Briefly, adult female mosquitoes that were between 0.5 and 3 h old, or adult females that were 5 days old, were intrathoracically injected ~0.2 μl 4% formaldehyde in PBS. Abdomens were then separated from the thorax, a coronal cut was made along one of the pleural membranes, and the abdomens were then pealed laterally such that the cuticle and associated tissues formed a continuous dorsal-pleural-ventral sheet. After incubating the abdomens in 4% formaldehyde in PBS for 2–6 h, tissues were washed in PBS, incubated in PBS containing 0.3% Triton X-100 (PBST), blocked in 10% normal goat serum in PBST for 2 h and incubated for 3 days in a PBST solution containing a rabbit anti-CCAP antibody (provided by H. Agricola, University of Jena, Germany; dilution 1:5000). Tissues were then washed in PBST, and incubated in a PBST solution containing goat anti-rabbit IgG antibody coupled to Cy3 (Jackson ImmunoResearch, West Grove, PA, USA; 1:5000 dilution). After immunolabeling, whole-mounts were washed in PBS and the musculature of some specimens was stained with phalloidin-AlexaFluor 488 (Invitrogen) as described previously (Glenn et al., 2010). After washing, abdomens were mounted on glass slides using Aqua Poly/Mount (Polysciences Co., Warrington, PA, USA).

Immunolabeling experiments were carried out with whole-mounts and sectioned tissues of the heads of 5-day-old mosquitoes. For whole-mounts, the proboscis was removed at its origin together with a piece of the head capsule. The resulting opening was enlarged with forceps and Bouin's fixative was injected into the head capsule using a glass microcapillary needle. The head was then carefully opened around the compound eyes, and immunolabeling was carried out as above. Because mounting of whole brains resulted in considerable tissue distortion, immunolabeling was also carried out in sectioned heads. For this, the head capsule was opened and aqueous Bouin's fixative was injected. The heads were then immersed in fixative for 2 h at 40°C, washed in PBS, injected with 40% sucrose in PBS and immersed in this solution overnight at 40°C. The heads were then embedded in tissue freezing medium (Electron Microscopy Sciences, Hatfield, PA, USA) in a mold with a copper block as base. Blocks were frozen in a solution of dry ice and acetone, and 20 μm thick cryosections were cut using a Leica CM1900 cryostat. Sections were transferred to gelatin-coated slides, air dried for 1 h and immunolabeled as above except that incubation and washing times were shorter.

Specimens were observed using a Zeiss LSM 510 META laser scanning confocal microscope. For whole-mounts, Z-stacks containing 15–22 optical slices were acquired in 0.6 μm intervals using Zeiss LSM 5 software, and projected to create a 2-D image. As negative labeling controls, omission of the primary antibody was performed, and this abolished all labeling. Specificity controls for this anti-CCAP primary antibody have been reported previously (Kostron et al., 1996; Woodruff et al., 2008; Honegger et al., 2011; Lee and Lange, 2011). In the present study, pre-absorption of a 1:1000 dilution of the anti-CCAP antibody with 10 μmol l^{-1} synthetic CCAP for 18 h at 4°C prior to being used in immunolabeling abolished all labeling.

RESULTS

Anopheles gambiae CCAP gene structure

The *A. gambiae CCAP* gene was identified by performing a TBLASTN search of the AgamP3 assembly of the genomic sequence (www.vectorbase.org) using the conserved CCAP peptide (Stangier et al., 1987; Lee et al., 2011) as the query sequence. This search revealed a single *CCAP* gene in *A. gambiae* (VectorBase ID: AGAP009729), which is located in chromosome 3R. To determine the *A. gambiae CCAP* transcript structure, the central region of the

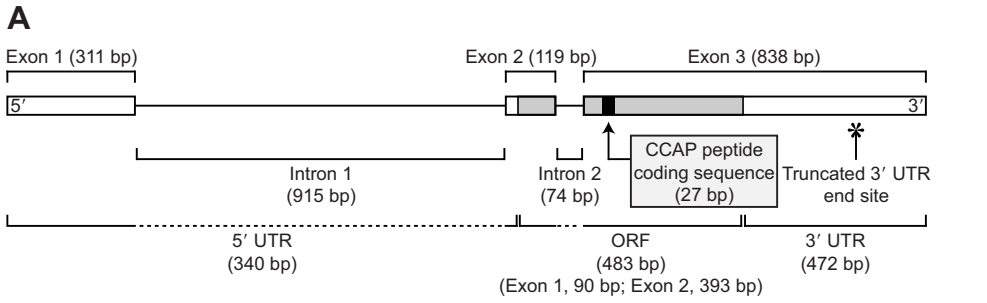

B

```
Anopheles gambiae       --MTHRTAAKLLLAVVSLFCVLQMLECGVVDRQPRAYKQYNTEP----------Q 43
Aedes aegypti           --MNSTAVTILLALAVTILCLAHVIDCGVVDREPRAYKQYSNEP---------PPA 45
Culex pipiens           --MSPTTVTSLFALTVAMAFFIHVIDCGVVDREPRAYKQYNTNSNTAGGGGEVPA 54
Drosophila melanogaster MRTSMRISLRLLALLACAICSQASLERENNEGTNMANHKLSGVIQWK-------YE 49
                                *                       *

Anopheles gambiae       KRPFCNAFTGCGKKRSSASSPPTAAAAAAAAAMLQRHLQTMDPGRKDRMGSDFDPNEESI 103
Aedes aegypti           KRPFCNAFTGCGKKRSSVVP-------VTPVNMIHRHALTSEQNRP-KVTEGFDPNEDSL 97
Culex pipiens           KRPFCNAFTGCGKKRSSVA--------VTPVAMMHRHALTSEQNRP-KVTEGFDPNEDSL 105
Drosophila melanogaster KRPFCNAFTGCGRKRTYPS--------YPPFSLFKRNEVEEKPYNN-------EYLSEGL 94
                        ************ **              *

Anopheles gambiae       SSLLDLNTEPAVEDLLRQIMSEAKLWEAIQEANREIYLQKSGMKDQRNDFPLTFSTQ---- 160
Aedes aegypti           ANLIDLNTEPAVEDLMRQIMSEAKLWEAIQEANREIYLQKQGQKSESNSFPISFSTQ---- 154
Culex pipiens           ANLIDLNTEPAVEDLMRQIMSEAKLWEAIQEANREIYLQKQGQKTQSDSFPISFSTQ---- 162
Drosophila melanogaster SDLIDINAEPAVENVQKQIMSQAKIFEAIKEASKEIFRQKNKQKMLQNEKEMQQLEERESK 155
                          * * * *****    **** **  *** **  **  **   *
```

Fig. 1. *Anopheles gambiae* CCAP gene structure, conceptual translation and alignment with other dipteran CCAP sequences. (A) *Anopheles gambiae* CCAP gene structure, marking the position and length of the 5′ and 3′ untranslated regions (UTRs), the three exons and the two introns, the open reading frame (ORF; spans an intron) and the location of the CCAP peptide coding sequence. During sequencing, two distinct 3′ UTR clones were identified. The larger clone is pictured and the end site of the shorter clone is marked with an asterisk. (B) Conceptual translation of *A. gambiae* CCAP (sequenced in this study; GenBank ID: JX880074) and alignment with the CCAP sequences of *Aedes aegypti* (XM_001649143), *Culex pipiens quinquefasciatus* (XM_001847811) and *Drosophila melanogaster* (NM_142826). The predicted signal peptides are in italics, the CCAP peptide is contained within the black box, the cleavage sites are underlined and the C-terminal glycine that is amidated is highlighted in bold. Asterisks denote residues that are conserved amongst all sequences.

transcript was sequenced using cDNA synthesized from the whole bodies of adult females and primers constructed using the genomic sequence as a reference. Then, the 5′ and 3′ ends of the *CCAP* transcript were sequenced from a 5′/3′ RACE library and primers that were constructed using the sequence of the central region of *CCAP* and the RACE vector sequence.

Assembly of the sequences revealed that the *CCAP* transcript is 1268 nucleotides (bp) in length, and is composed of a 340 bp 5′ untranslated region (UTR), a 483 bp open reading frame (ORF; encompasses two exons where the coding sequences are 90 and 393 bp in length) and a 445 bp 3′ UTR (Fig. 1A; GenBank ID: JX880074). Alignment of the mRNA sequence and the chromosome 3R genomic sequence revealed that the *CCAP* gene is composed of exons that are 311, 119 and 838 bp in length, introns that are 915 and 74 bp in length, and splice sites that are located within the 5′ UTR and within the ORF (located 5′ of the sequence coding the CCAP peptide). During 3′ RACE two distinct clones were sequenced, with the only difference being the length of the 3′ UTR. The larger clone yields the 1268 bp transcript and contains a classical AATAAA polyadenylation signal sequence (nucleotides 1241–1246) while the smaller clone yields a 1095 bp transcript that does not contain a polyadenylation signal sequence. Polyadenylation signal sequences have been reported for some insect *CCAP* genes (Park et al., 2003; Sakai et al., 2004) but not others (Loi et al., 2001; Lee et al., 2011), and perhaps truncation of the 3′ UTR is responsible for these observations.

Conceptual translation of the full-length mRNA revealed that *A. gambiae CCAP* encodes a 160 amino acid (aa) protein with a predicted mass of 17.9 kDa (Fig. 1B). The ORF encodes a 25 aa signal peptide, the CCAP peptide and multiple putative cleavage sites composed of dibasic amino acid residues (Veenstra, 2000). Based on empirical and bioinformatic experiments detailed in previously published work (Stangier et al., 1987; Cheung et al., 1992; Veenstra, 2000), cleavage from the signal peptide is followed by cleavage at the KR and KKR sequences that flank the CCAP peptide, yielding a sequence of H-PFCNAFTGCG. The C-terminal glycine is then amidated (Stangier et al., 1987; Cheung et al., 1992), yielding a mature CCAP sequence of H-PFCNAFTGC-NH_2.

Alignment of the CCAP full-length protein sequence with other dipteran CCAP protein sequences revealed perfect conservation of the CCAP peptide sequence, and near-perfect conservation of the predicted cleavage sites (Fig. 1B). Further alignment of the mosquito CCAP peptide with CCAP peptides across the phylum Arthropoda revealed that *A. gambiae* CCAP is 100% conserved with all known arthropod CCAP peptides with the exception of *D. pulex* (Dircksen et al., 2011; Lee et al., 2011). Outside of the CCAP peptide region, considerable conservation between dipteran CCAPs was only observed between amino acids 97 and 138 (57% identity). Given that *CCAP* is not known to produce any other bioactive peptides, it is possible that this second conserved region is required for the proper processing of the CCAP peptide.

Developmental expression of *CCAP* and *CCAPR*

Quantitative RT-PCR analyses of *CCAP* transcription in the whole bodies of mosquitoes at different developmental stages revealed that *CCAP* is primarily expressed in the immature stages, but that mRNA levels remain elevated in adults relative to eggs (Fig. 2A). Specifically, relative to eggs, *CCAP* mRNA levels increase eightfold in second instar larvae, are decreased by half in third instar larvae and then increase to maximum levels in the late, black pupa stage (33-fold increase relative to eggs). At 24 h following eclosion, *CCAP* levels drop to threefold higher than eggs and remain near this level until the 10th day following adult emergence, which was the last time point assayed.

Because *CCAP* activity is dependent on its binding to a receptor, we then tested whether expression of the CCAP receptor (*CCAPR*) mirrored expression of *CCAP*. A bioinformatic analysis of the *A. gambiae* genomic sequence revealed a single *CCAPR* (AGAP001962), and this G protein-coupled receptor has been previously shown, using a heterologous expression system, to have

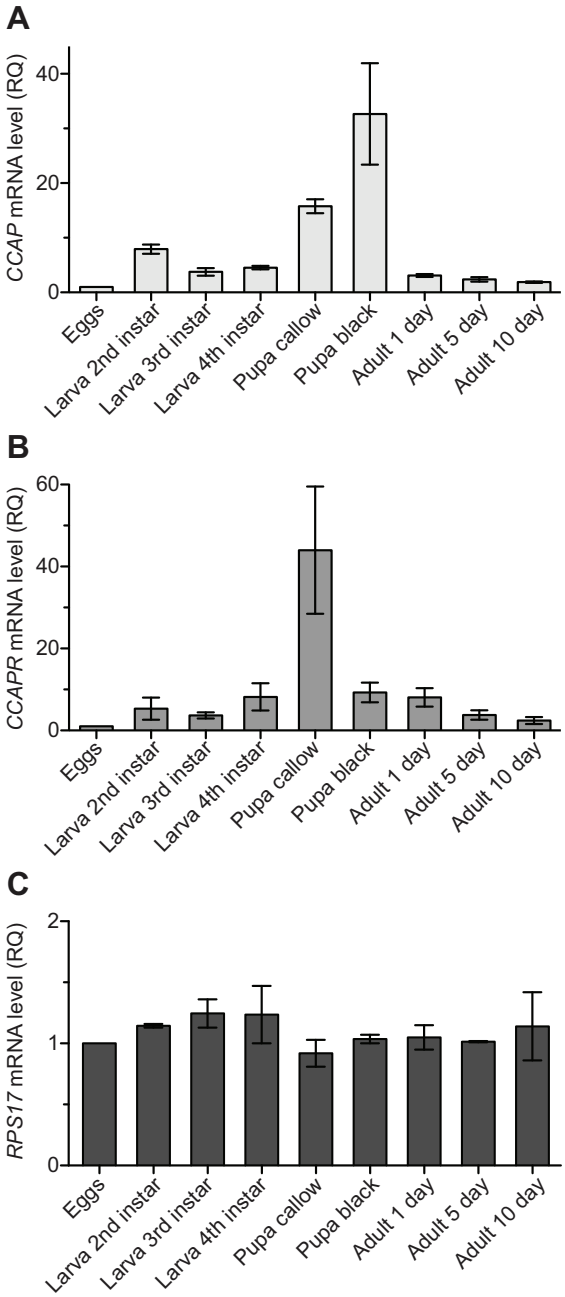

Fig. 2. *Anopheles gambiae* CCAP and CCAP receptor (CCAPR) developmental expression. Quantitative RT-PCR analysis of the transcription of *CCAP* (A), *CCAPR* (B) and *RPS17* (C) in eggs with developing first instar larvae, second through fourth instar larvae, callow (early) and black (late) pupae, and adults at 24 h, 5 days and 10 days after eclosion. The graph displays the mean ± s.e.m. fold-difference in mRNA levels relative to eggs (relative quantification; RQ), using *RPS7* as the reference gene. Peak expression for both CCAP and CCAPR occurs during the pupal stage. *RSP17* mRNA levels are constant throughout development.

strong affinity for the CCAP peptide (Belmont et al., 2006). In preparation for *CCAPR* transcriptional analyses, an 806 kb region of *A. gambiae CCAPR* was amplified by PCR and sequenced (not shown). After confirming sequence identity with the published sequence of *A. gambiae* bioactive *CCAPR* (Belmont et al., 2006), primers were constructed for qPCR and dsRNA synthesis (see below). Transcriptional analyses revealed that expression of *CCAPR* largely mirrors expression of *CCAP* (Fig. 2B). Relative to eggs, *CCAPR* mRNA levels increase fivefold in second instar larvae, drop slightly in third instar larvae and then increase to maximum levels in the early, callow pupa stage (44-fold increase relative to eggs). As the pupae develop and eclose, mRNA levels decrease but remain elevated relative to eggs.

Finally, to validate *RPS7* as the reference gene, we also measured mRNA levels of the housekeeping gene *RPS17* (Fig. 2C). Statistical analyses of the transcriptional data by one-way ANOVA revealed that although mRNA levels of *CCAP* (P<0.0001) and *CCAPR* (P=0.001) change significantly with life stage, mRNA levels of *RPS17* do not change as mosquitoes develop (P=0.7259).

Transcription of *CCAP* and *CCAPR* in different body regions

Quantitative RT-PCR analyses of *CCAP* transcription in the head, thorax and abdomen suggest that in older mosquitoes, *CCAP* is primarily transcribed in the brain (Fig. 3A). Overall, the whole bodies of newly emerged mosquitoes have 17 times the amount of *CCAP* mRNA than their older counterparts. The heads of both young and old mosquitoes are enriched in *CCAP* mRNA, although relative levels of *CCAP* mRNA are eightfold higher in young mosquitoes. Of all body segments, the abdomens of old mosquitoes have the lowest amount of *CCAP* mRNA, which is greater than 100-fold lower than *CCAP* mRNA levels in the abdomens of newly eclosed mosquitoes. Statistical analysis of these data by two-way ANOVA showed that *CCAP* mRNA levels change with age (P=0.0004) and body segment (P<0.0001), and that *CCAP* mRNA distribution across the different body segments changes with age (interaction; P<0.0001).

Because the action of the CCAP peptide on cardiac musculature is dependent on its binding to the CCAP receptor, we then measured whether the CCAP receptor was also transcribed in <1-h- and 5-day-old mosquitoes (Fig. 3B). Similar to *CCAP*, transcription of *CCAPR* is enriched in newly emerged mosquitoes. Specifically, the whole bodies of <1-h-old adults have four times the amount of *CCAPR* mRNA than older mosquitoes. Within the different body segments, *CCAPR* mRNA is also enriched in the head, but significant transcription was detected in all body regions. Statistical analysis of these data by two-way ANOVA showed that *CCAPR* mRNA levels change with age (P=0.0083) and body segment (P<0.0001), and that *CCAPR* mRNA distribution across the different body segments changes with age (interaction; P<0.0001).

Finally, to validate *RPS7* as the reference gene, we also measured mRNA levels of the housekeeping gene *RPS17* (Fig. 3C). Statistical analysis of these data by two-way ANOVA showed that *RPS17* mRNA levels do not change with age (P=0.3433) or body segment (P=0.5548), and that *RPS17* mRNA distribution across the different body segments does not change with age (interaction; P=0.4162).

CCAP injection increases heart contraction rates

Analysis of videos taken before mosquitoes received any treatment revealed that the heart contracts at an average rate of 1.90 Hz (Fig. 4). When divided by contraction direction, the heart contracts at 1.92 Hz in the anterograde direction and 1.84 Hz in the retrograde direction. The heart reverses contraction direction 10.5 times per minute and spends 76% of the time contracting anterograde (toward the head) and 24% of the time contracting retrograde (toward the posterior abdomen). Similarly, 76% of the contractions propagate in the anterograde direction and 24% of the contractions propagate in the retrograde direction.

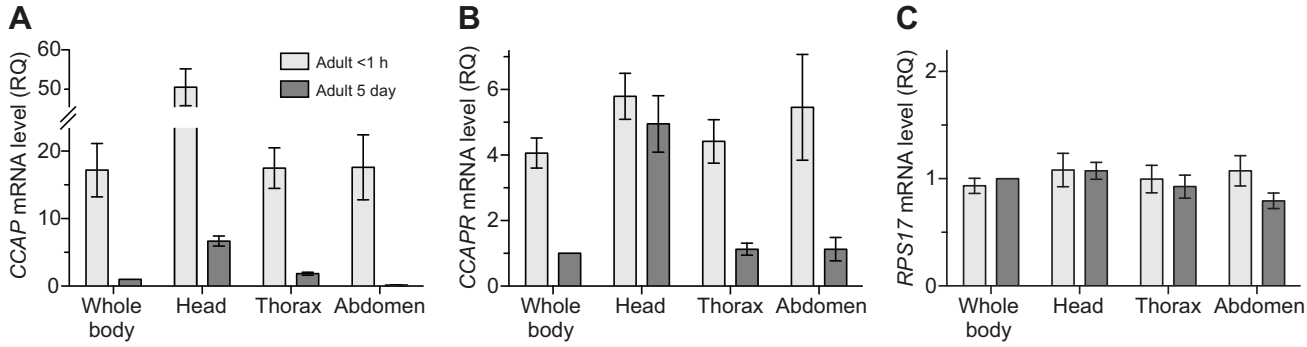

Fig. 3. *Anopheles gambiae* CCAP expression in different body segments. Quantitative RT-PCR analysis of *CCAP* (A), *CCAPR* (B) and *RPS17* (C) mRNA levels in the whole bodies, heads, thoraces and abdomens of adult mosquitoes that are <1 h and 5 days old. The graphs display the mean ± s.e.m. fold-difference in mRNA levels relative to 5-day-old whole bodies (relative quantification; RQ), using *RPS7* as the reference gene. For CCAP and CCAPR, peak expression occurs in the heads of mosquitoes at <1 h post-eclosion. *RPS17* mRNA levels do not change relative to the *RPS7* reference.

Comparison of videos taken before and after treatment showed that CCAP increases heart contraction rates in a dose-dependent manner (Fig. 4A–C, Fig. 5). Injection of PBS increases the total heart contraction rate by 7%, but injection of CCAP between the concentrations of 1×10^{-5} and 1×10^{-7} mol l^{-1} increases the total heart contraction rate by 21–26%. When divided by contraction direction, PBS injection increases the anterograde and retrograde contraction rates by 7 and 5%, respectively, but injection of CCAP between the concentrations of 1×10^{-5} and 1×10^{-7} mol l^{-1} increases the anterograde and retrograde contraction rates by 24–28 and 16–23%, respectively. Analysis of the raw data by repeated-measures two-way ANOVA detected a highly significant interaction between CCAP dose and a change in heart rate (P<0.0001 for total, anterograde and retrograde; Fig. 4), and this dose-dependent effect was confirmed by Kruskal–Wallis analysis of the ratios of heart contraction rates post- and pre-treatment (P<0.0001 for total, anterograde and retrograde; Fig. 5). Visual analysis of the ratio data as well as Dunn's multiple comparison tests showed that the largest CCAP-mediated cardioacceleratory effect occurs after injection of doses between 1×10^{-5} and 1×10^{-7} mol l^{-1} (P<0.0001 for total, anterograde and retrograde). This dose-dependent effect, while consistent for all heart rate measurements, was more pronounced during periods of anterograde heart contractions, a finding consistent with a report in *Drosophila melanogaster* that suggests that CCAP may function as an anterograde pacemaker (Dulcis et al., 2005). Overall, the weakest effects of CCAP treatment on contraction rates were observed at the lowest and highest CCAP concentrations. The weak or non-existent effect seen at 1×10^{-10} mol l^{-1} CCAP is likely due to insufficient activation of the CCAP receptor, and low bioactivity of CCAP when applied at 1×10^{-4} and 1×10^{-3} mol l^{-1} is likely due to desensitization of the receptor. Reductions in the cardioacceleratory activity of CCAP at both high and low concentrations have been reported in other insects (Ejaz and Lange, 2008; da Silva et al., 2011; Lee and Lange, 2011).

Although CCAP increases heart contraction rates, treatment with this neuropeptide does not affect any of the other measured parameters (Fig. 4D–H). Repeated-measures two-way ANOVA did not detect a dose-dependent effect of CCAP treatment on the percentage of contractions propagating in the anterograde or retrograde directions or on the percentage of time the heart spends contracting in the anterograde and retrograde directions (P≥0.5434 for all). Likewise, Sidak's multiple comparisons did not detect a significant difference between the pre-treatment and post-treatment groups for any of these parameters. However, as we have shown before (Hillyer et al., 2012), the process of injection leads to a consistent decrease in the frequency of heartbeat directional reversals, but no interaction between CCAP dose and this decrease was detected (P=0.6514). Thus, CCAP has a cardioacceleratory effect, but does not modulate contraction direction or the frequency of heartbeat directional reversals.

CCAP injection increases cardiac hemolymph velocity

Given that CCAP increases heart contraction rates, we hypothesized that this increase leads to an increase in hemolymph flow velocity within the heart lumen. To test this, the velocity of intrathoracically injected neutral density fluorescent microspheres was measured as they traveled through the heart lumen after treatment with either PBS or 1×10^{-7} mol l^{-1} CCAP in PBS. Measurements of hemolymph flow velocity revealed that 10 min after injection with PBS, hemolymph in the heart lumen is propelled at 6690 μm s^{-1} (±1764 s.d.) in the anterograde direction and 5805 μm s^{-1} (±2051 s.d.) in the retrograde direction (Fig. 6). When CCAP was injected instead of PBS, hemolymph velocity increased by 29% (8634±2392 μm s^{-1}) and 33% (7707±2436 μm s^{-1}) in the anterograde and retrograde directions, respectively. Thus, CCAP significantly increases hemolymph flow velocity (P<0.0001 for both; Fig. 6).

CCAP knockdown decreases the total and anterograde heart contraction rates

In order to corroborate that CCAP has cardioacceleratory activity, RNAi-based experiments were performed where *CCAP* was knocked down using two different dsRNA fragments, or where *CCAP* and *CCAPR* were simultaneously knocked down. The average *CCAP* knockdown efficiency for the five independent trials was 57%, and the single trial that also knocked down *CCAPR* did so at an efficiency of 61%.

Four days after injection of the control dsRNA, *bla(Ap^R)*, the mosquito heart contracted at rates of 1.91, 1.91 and 1.87 Hz in the total, anterograde and retrograde directions, respectively (Fig. 7). The heart reversed contraction direction 11.4 times per minute and spent 75 and 25% of the time contracting in the anterograde and retrograde directions, respectively. Similarly, 75% of the contractions propagated in the anterograde direction while 25% of the contractions propagated in the retrograde direction. These data show that mosquitoes injected with *bla(Ap^R)* dsRNA have virtually identical heart physiology as untreated mosquitoes (Fig. 4), thus validating this dsRNA as an appropriate control for RNAi experiments.

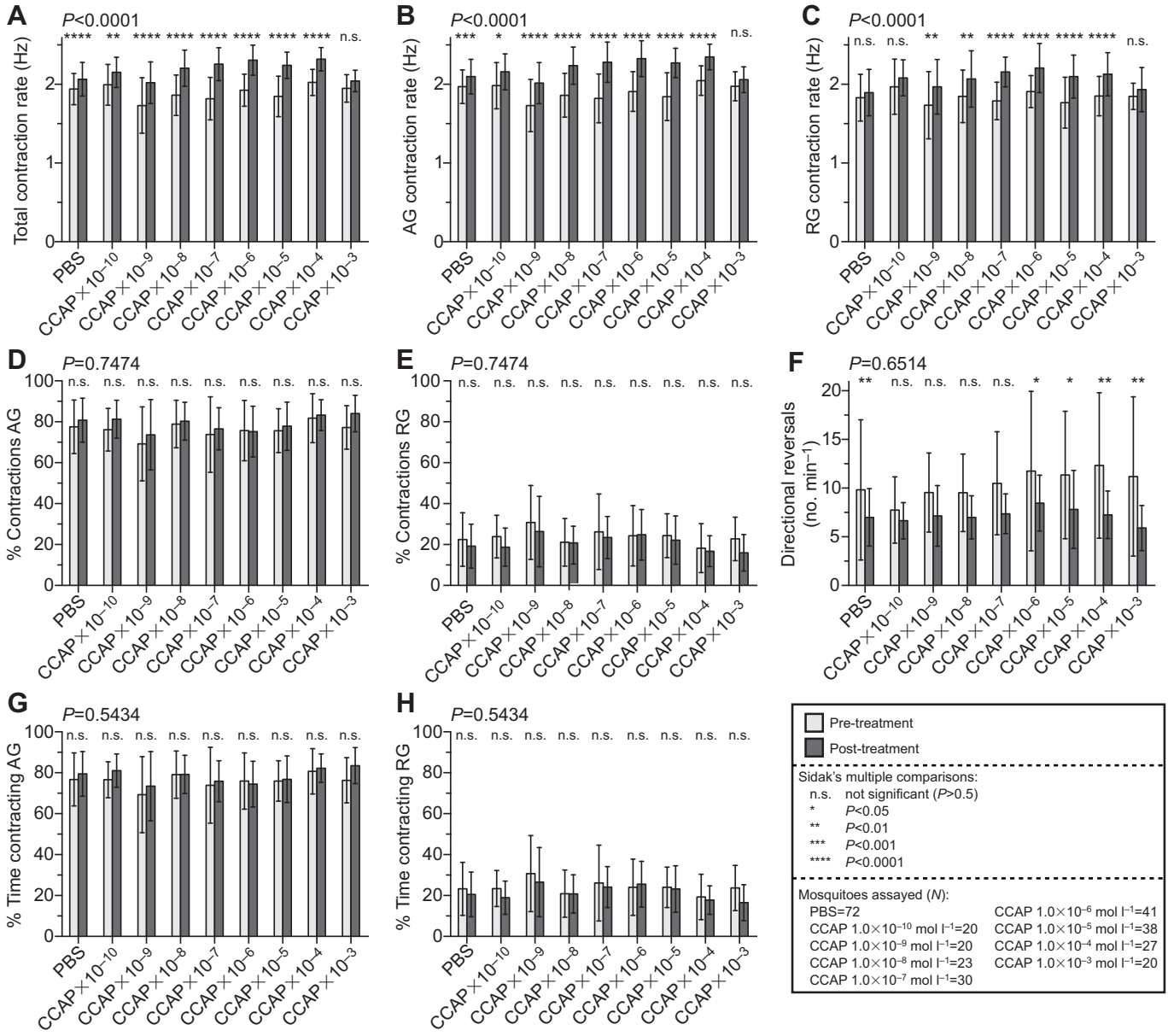

Fig. 4. Effect of CCAP injection on mosquito heart physiology. Heart physiological recordings were acquired before (pre) and after (post) treatment with CCAP doses ranging from 0 mol l^{-1} (PBS) to 1×10^{-3} mol l^{-1} (diluted ~1:5 upon injection). Columns summarize the raw data, with the heights marking the mean and the whiskers denoting the standard deviation. The single *P*-value at the top of each graph compares the pre- and post-treatment raw data sets using repeated-measures two-way ANOVA, and shows whether there is an interaction between CCAP dose and changes in heart physiology. The *P*-value above each pair of columns compares the data before and after treatment for each CCAP dose (0 to 1.0×10^{-3} mol l^{-1}) using Sidak's *post hoc* tests. Heart parameters measured were the total, anterograde (AG) and retrograde (RG) contraction rates (A–C), the percentage of contractions propagating in the anterograde and retrograde directions (D,E), the frequency of heartbeat directional reversals (F) and the percentage of time spent contracting in the anterograde and retrograde directions (G,H). Sample sizes and abbreviations are detailed in the box at the bottom right of the figure. Overall, CCAP injection increases the heart contraction rate.

Relative to the *bla(Ap^R)* dsRNA controls, silencing *CCAP* transcription resulted in a statistically significant 6 and 7% reduction in the total (P=0.0080) and anterograde (P=0.0066) heart contraction rates, respectively (Fig. 7A,B). However, *CCAP* knockdown led to a non-statistically significant 4% decrease in the retrograde contraction rate (P=0.1924; Fig. 7C), and *CCAP* knockdown had no effect on the percent of time or contractions propagating in the anterograde and retrograde directions, or in the rate of heartbeat directional reversals ($P\geq0.3229$ for all; Fig. 7D–H). Thus, knockdown of CCAP decreases heart contraction rates.

In older adults, the CCAP peptide is primarily detected in the head region

In a study that focused on bursicon expression in the mosquito ventral nerve cord, we recently showed that the paired neurons 27 and IN704 homologues co-expressing bursicon and CCAP undergo apoptosis by 24 h post-eclosion, and that no additional CCAP immunoreactive (CCAP-IR) neurons were present in the abdominal ganglia (Honegger et al., 2011). Because peripheral neurosecretory cells expressing CCAP have been described in *Drosophila* (Dulcis and Levine, 2003), we expanded on our previous work by assessing

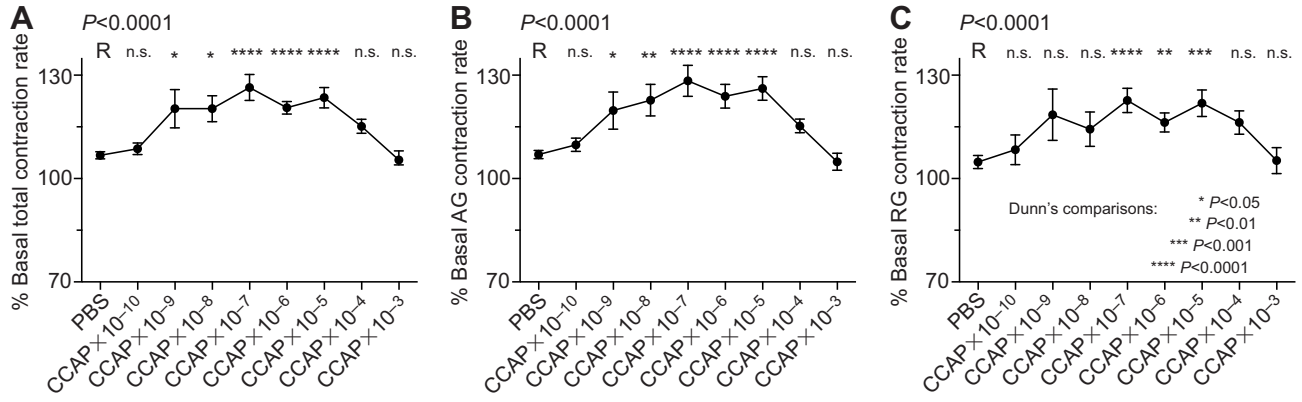

Fig. 5. Effect of CCAP injection on mosquito heart rates. For each individual, the effect of treatment on total (A), anterograde (B) and retrograde (C) contraction rates was calculated by dividing the post-treatment values by the pre-treatment values. Data are presented as means ± s.e.m., and each data set was analyzed using the Kruskal–Wallis test. Multiple comparisons were made using the Dunn's test, with the *P*-values displaying the comparison of each CCAP dose against the PBS reference (R) group. Overall, CCAP injection increases the heart contraction rate.

the presence of CCAP in both the ventral and dorsal abdomen of older mosquitoes. Analysis of the dorsal, ventral and pleural regions of the abdomen of 5-day-old mosquitoes failed to detect CCAP in the central ganglia, neuronal projections or any other tissues (Fig. 8A,B). As a positive control, we performed the same experiment using abdomens from adult mosquitoes that were 0.5 to 3 h old at the time of fixation (Fig. 8C,D). As expected, CCAP was strongly detected in the somata of neurons 27, located in the abdominal ganglia of the ventral nerve cord (Fig. 8C). Moreover, we also detected CCAP in peripheral projections that arise from neurons 27. These projections span the pleuron, extend across the alary muscles and onto the heart (Fig. 8D). No peripheral CCAP-IR neurons were detected in young or old adults.

Because at 5 days post-eclosion the majority of *CCAP* mRNA was detected in the head region (Fig. 3), we investigated whether the CCAP peptide could be detected in the brain and associated tissues. CCAP immunolabeling of serial frozen brain sections consistently detected CCAP-IR in approximately five neurons of the anterior-lateral protocerebrum (pars lateralis) and one to two neurons of the posterior protocerebrum (Fig. 9A). These experiments also detected CCAP-IR in the lateral protocerebrum at the border with the optic lobe (lobula) and the distal part of the medulla (not shown). The positions of these somata are similar to those shown recently in fifth instar *Rhodnius prolixus* (Lee and Lange, 2011). In addition, immunolabeling of sectioned tissues and whole mounts showed strong CCAP-IR in a bilateral cluster of cells in the subesophageal ganglion and in projections in the corpora cardiaca (CC; Fig. 9B,C). Faint CCAP-IR was also detected in fiber tracts in the nervi corpora cardiaca 2 (NCC2) that connect the brain with the CC, suggesting that neurons in the pars lateralis project into the CC (Fig. 9C). Finally, projections in the neck region were intensely CCAP-IR (not shown), and these projections seemed to comprise the surface layers of the esophagus as part of the retrocerebral complex. These data suggest that CCAP exerts its cardioacceleratory effect through its release into the hemocoel by neurons in the brain and subesophageal ganglion.

DISCUSSION

CCAP is a pleiotropic nonapeptide that is produced by crustaceans, hexapods and chelicerates. Among its many described functions, CCAP has myotropic activity, which is manifested by the stimulation of heart (Furuya et al., 1993; Lehman et al., 1993; Dulcis et al., 2005; Wasielewski and Skonieczna, 2008; da Silva et al., 2011) and visceral muscle contractions (Donini et al., 2001; Sakai et al., 2004). In mosquitoes, both *CCAP* and *CCAPR* have been identified (Riehle et al., 2002; Belmont et al., 2006), but the function of this peptide–receptor combination in the culicid lineage has not been described. Here, we elucidated the CCAP gene structure, determined the developmental expression pattern of *CCAP* and its receptor and showed that CCAP has potent cardioacceleratory activity in the malaria mosquito *A. gambiae*. To our knowledge, this is the first description of a mosquito factor (protein, peptide or transmitter) that regulates mosquito circulatory physiology, and the first description of increased hemolymph velocity following CCAP treatment in an undissected insect.

CCAP was originally discovered because of its cardioacceleratory activity in the shore crab, *C. maenas* (Stangier et al., 1987). Since, this highly conserved nonapeptide has been shown to have cardioacceleratory activity in insects of the orders Diptera (Nichols et al., 1999; Dulcis et al., 2005), Coleoptera (Wasielewski and Skonieczna, 2008), Hemiptera (Lee and Lange, 2011), Lepidoptera

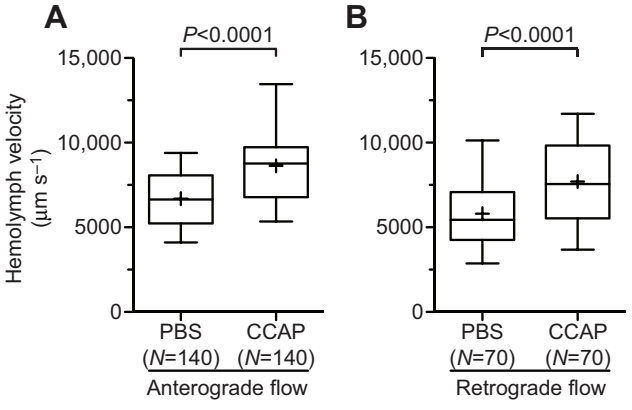

Fig. 6. Effect of CCAP injection on cardiac hemolymph flow velocity. Tracking of red fluorescent microspheres as they travel in the anterograde (A) and retrograde (B) directions following treatment with PBS or 1×10^{-7} mol l^{-1} CCAP in PBS. Plots show the mean (+), median (center line), 50% of the data (box) and 95% of the data (whiskers). *P*-values comparing the data from PBS- and CCAP-treated mosquitoes result from Mann–Whitney tests. Overall, CCAP treatment increases hemolymph flow velocity.

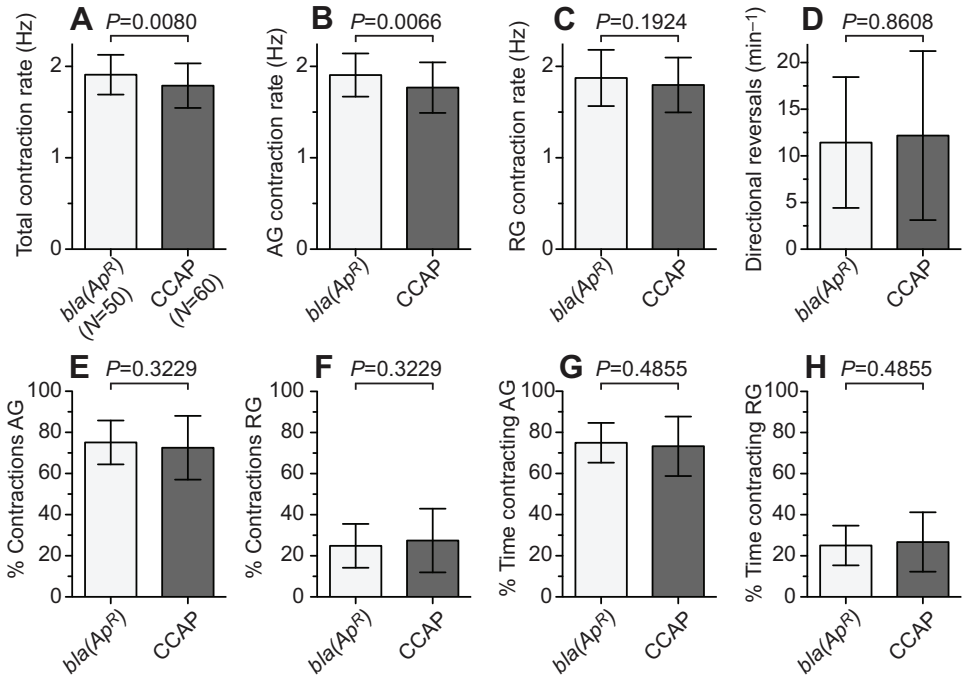

Fig. 7. Effect of CCAP gene knockdown on mosquito heart physiology. In each graph, the left column shows heart physiology in mosquitoes injected with *bla(Ap^R)* dsRNA (control) and the right column shows heart physiology in mosquitoes for which transcription of CCAP was knocked down. Column heights mark the mean and whiskers denote the standard deviation. *P*-values comparing the data of control and experimental mosquitoes result from unpaired *t*-tests. Heart parameters measured were the total, anterograde (AG) and retrograde (RG) contraction rates (A–C), the frequency of heartbeat directional reversals (D), the percentage of contractions propagating in the anterograde and retrograde directions (E,F) and the percentage of time spent contracting in the anterograde and retrograde directions (G,H). Sample sizes: *bla(Ap^R)* controls, 50; CCAP knockdown, 60. Overall, lowering CCAP levels significantly reduces the total and anterograde heart contraction rates.

(Lehman et al., 1993; Dulcis et al., 2001) and Phasmatodea (Ejaz and Lange, 2008; da Silva et al., 2011). In these insects, the reported increases in heart rates following exogenous CCAP exposure range from 19% (Nichols et al., 1999) to 380% (Lee and Lange, 2011), and the CCAP doses that yield the most pronounced increases in heart rates range from 1×10^{-10} moll^{-1} (Lee and Lange, 2011) to 1×10^{-3} moll^{-1} (Lehman et al., 1993). The reasons for the broad differences in CCAP myotropic activity are not clear, but the cardioacceleratory effect of this neuropeptide appears to be lower (reduced activity even at higher concentrations) in the superorder Endopterygota (orders Diptera, Lepidoptera and Coleoptera) when compared with the superorders Polyneoptera (Phasmatodea) or Paraneoptera (Hemiptera). Although this evolutionary trend is clear, it is equally plausible that the differences observed do not have an evolutionary origin, and that instead are due to the different methodologies used. For example, in *D. melanogaster*, CCAP has a significantly higher cardioacceleratory effect in dissected flies when compared with intact flies (Nichols et al., 1999). The present study and that of Nichols et al. (Nichols et al., 1999) are the only studies that have measured the cardioacceleratory activity of CCAP in a true *in vivo* context, without the dissection of the outer cuticle and the immersion of the dorsal vessel in a non-hemolymph solution.

In the present study we conclusively show that CCAP increases heart contraction rates by up to an average of 28%, which is the first such report in a dipteran insect of the suborder Nematocera. In brachyceran dipterans, a cardioacceleratory function for CCAP has been described for the fruitfly *D. melanogaster*. Specifically, Nichols et al. (Nichols et al., 1999) showed that injection of CCAP increased the adult heart rate by 19%. Then, Dulcis et al. (Dulcis et al., 2005) showed that targeted ablation of CCAP-producing neurons, but not CCAP silencing by RNAi, decreases heart rates by 37–51%. Furthermore, the differences observed between anterograde and retrograde heart rates suggested that CCAP may regulate the anterograde pacemaker (Dulcis et al., 2005), data that are consistent with the higher effect that CCAP appears to have during mosquito anterograde contraction periods. However, heart physiology between *Drosophila* and mosquitoes is significantly different: although anterograde and retrograde contraction rates are similar in mosquitoes (Andereck et al., 2010; Glenn et al., 2010; Hillyer et al., 2012), heart rates in *Drosophila* change with contraction direction, although the magnitude and directionality of these changes has not been consistent between studies (Dulcis et al., 2005; Wasserthal, 2007). Thus, the study presented herein shows that while nematoceran and brachyceran cardiac physiology is markedly different, at least some of the peptidergic signals that maintain heart rhythms are shared between the two major dipteran lineages.

During development, peak expression of *CCAP* and *CCAPR* occurs in second instar larvae and pupae. We have observed that peak expression of the neurohormones bursicon and corazonin also occurs in the immature stages, and corazonin's expression pattern matches *CCAP*'s bimodal distribution in that it contains peaks in second instar larvae and pupa (Honegger et al., 2011; Hillyer et al., 2012). There are several commonalities between CCAP, bursicon and corazonin, with the primary one being their functional role in several aspects of the molting process. Specifically, CCAP and bursicon are key players in ecdysis and cuticular tanning (Arakane et al., 2008; Honegger et al., 2008; Lahr et al., 2012). The role of corazonin in molting is less clear (Veenstra, 2009; Boerjan et al., 2010), but this neurohormone regulates the melanization patterns associated with the gregarious phase of migratory locusts (Tawfik

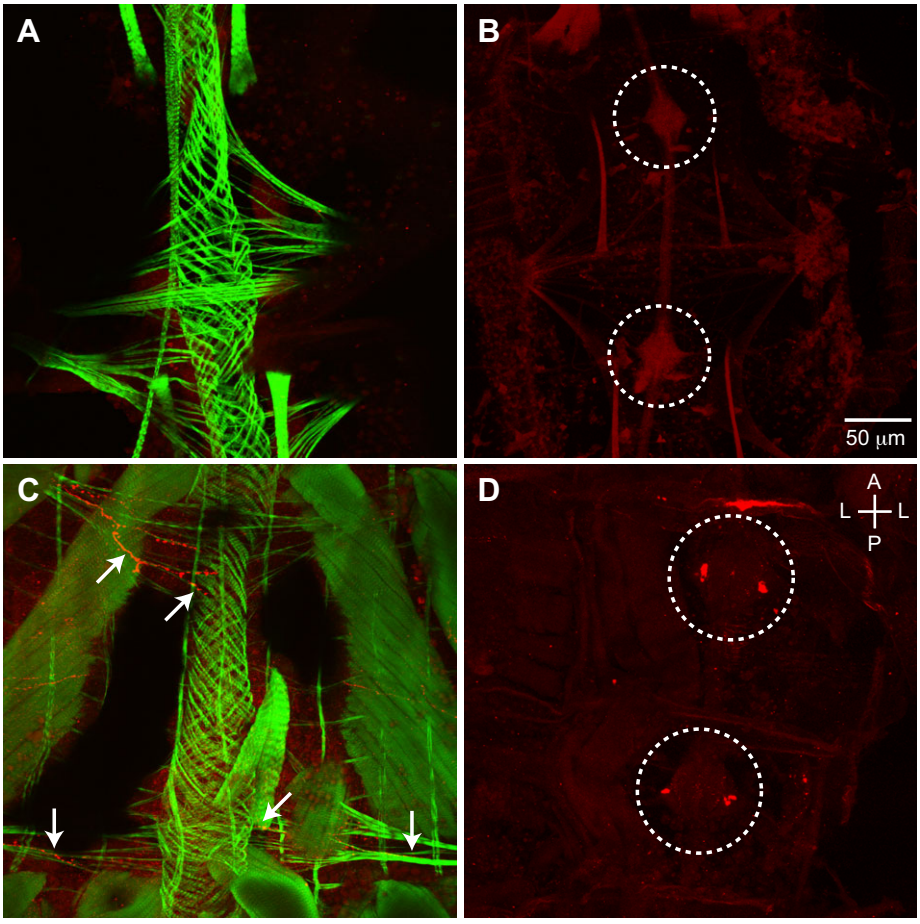

Fig. 8. CCAP immunohistochemistry in the mosquito abdomen. The dorsal (A,C) and ventral (B,D) regions of abdomens from 5-day-old (A,B) and <1-h-old (C,D) adult mosquitoes were visualized following CCAP (red; anti-CCAP antibody) and muscle (green in A,B; phalloidin) labeling. No CCAP immunoreactivity was seen in the abdomens of 5-day-old mosquitoes, but strong CCAP labeling of neurons 27 (within the circled abdominal ganglia in D; similar locations are marked in B) as well as projections innervating muscle tissue (e.g. arrows), including the heart, were detected in newly emerged mosquitoes. A, anterior; L, lateral, P, posterior.

et al., 1999). Given the role these neurohormones play in molting, it is not surprising that their mRNA levels drop after adult ecdysis, the final molting event. Accordingly, in lepidopterans and coleopterans there is a reduction in *CCAP* and *CCAPR* mRNA levels after emergence (Loi et al., 2001; Arakane et al., 2008; Li et al., 2011). This developmental pattern is similar in mosquitoes, and the complementary approaches used in this study show that CCAP plays a cardioacceleratory role in the adult stage: injecting the peptide increase the heart rate, but reducing endogenous CCAP levels by RNAi has the opposite effect. Thus, although this study did not attempt to uncover other possible functions for this pleiotropic neuropeptide in culicids, we show here that CCAP has a biologically meaningful cardioacceleratory role in the adult stage of *A. gambiae*. This represents the first report where specifically reducing endogenous *CCAP* expression leads to a reduction in cardiac output. The only other study that reported a similar effect accomplished this phenotype by ablating the CCAP-producing neurons – thus eliminating other neuropeptides and transmitters they

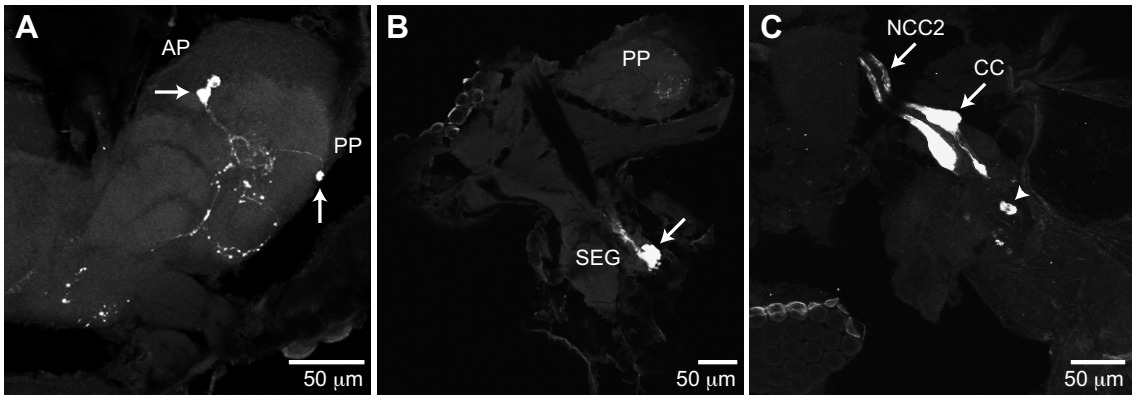

Fig. 9. CCAP immunohistochemistry in the mosquito head. (A) Oblique coronal section through the protocerebrum, showing a cluster of CCAP-immunoreactive (CCAP-IR) somata (arrows) in the anterior protocerebrum (AP) and a single soma on the posterior protocerebrum (PP) with intensely labeled arborizations. (B) Section through the subesophageal ganglion (SEG) showing intense CCAP-IR in a neuronal cluster with projections extending toward the PP. (C) Whole-mount showing intense CCAP-IR in the corpora cardiaca (CC), the nervi corpora cardiaca 2 (NCC2) and somata possibly located in the SEG (arrowhead). CCAP labeling in the NCC2 was significantly lower than labeling in the CC.

produce – and not by specific knockdown of *CCAP* (Dulcis et al., 2005).

Although we detected *CCAP* mRNA in the whole bodies of mosquitoes at all life stages, immunohistochemical analyses detected CCAP in the abdomens of freshly eclosed mosquitoes but not in the abdomens of mosquitoes at 5 days post-eclosion. We have previously shown that in newly eclosed mosquitoes, CCAP is highly expressed in neurons 27 and IN704 of the ventral nerve cord, but that these neurons undergo apoptosis by 12 h post-eclosion (Honegger et al., 2011). This is similar to what has been reported for *Manduca sexta* immatures (Ewer et al., 1998; Davis et al., 2001). In the present study we show that in newly eclosed mosquitoes, neurons 27 extend numerous peripheral projections that span the pleuron and innervate the alary and cardiac muscles, as is also seen in *M. sexta* and *Baculum extradendatum* (Davis et al., 2001; Ejaz and Lange, 2008). In *D. melanogaster*, additional peripheral neurons produce CCAP after eclosion and their projections innervate to the heart (Dulcis et al., 2005). Although we failed to detect CCAP in the abdomen of 5-day-old mosquitoes, gene expression data suggested that at this age the majority of CCAP is produced in the head. Immunocytochemical analyses confirmed the transcriptional data, and further showed that CCAP is present in specific neurons of the brain and subesophageal ganglion, and that projections from these neurons extend into the CC. This finding is largely in agreement with data on the distribution of CCAP in *Rhodnius prolixus* immatures (Lee and Lange, 2011). Thus, given that in older adults *CCAP* mRNA levels as well as CCAP-IR are highest in the head and lowest in the abdomen, these data suggest that CCAP reaches the heart and exerts its cardioacceleratory activity after being released into the hemocoel by neurons in the head region.

Finally, the physiological data presented herein are in agreement with our published data on basal mosquito heart physiology (Andereck et al., 2010; Glenn et al., 2010; Hillyer et al., 2012), with one possible exception. We previously reported that hemolymph flows through the mosquito heart at an average velocity of 8 mm s^{-1}, regardless of contraction direction (Glenn et al., 2010). In the present study, we measured hemolymph flow at velocities of 6.7 mm s^{-1} in the anterograde direction and 5.8 mm s^{-1} in the retrograde direction. Although the reason behind the difference between the two studies is not clear, possibilities include (1) that the experiments presented here employed two injections that were 10 min apart while the other study employed a single injection, (2) that the two studies used different mosquito strains (SUA2La hybrid *versus* G3), and (3) and that the mosquitoes used could have differed in their feeding/reproductive states. Regardless, this observed dissimilarity does not affect the conclusions of this study, as large and significant differences were observed between the control and CCAP-injected groups.

In summary, in this study we used complementary approaches to show that CCAP has potent cardioacceleratory activity in mosquitoes. By both increasing and decreasing CCAP levels in the hemocoel, we show that this peptide increases heart rates and hemolymph flow velocity. Thus, while CCAP expression decreases after adult ecdysis, the continued production of CCAP maintains elevated heart rates, and thus the mosquito heart is under partial neuronal control.

ACKNOWLEDGEMENTS

We are grateful to Dr Kendal Broadie for allowing the use of the Zeiss LSM 510 META confocal microscope and Dr David McCauley for allowing the use of the ABI 7300 RT-PCR System.

FUNDING

This research was funded by the National Science Foundation [grant number IOS-1051636 to J.F.H.].

REFERENCES

Andereck, J. W., King, J. G. and Hillyer, J. F. (2010). Contraction of the ventral abdomen potentiates extracardiac retrograde hemolymph propulsion in the mosquito hemocoel. *PLoS ONE* **5**, e12943.

Arakane, Y., Li, B., Muthukrishnan, S., Beeman, R. W., Kramer, K. J. and Park, Y. (2008). Functional analysis of four neuropeptides, EH, ETH, CCAP and bursicon, and their receptors in adult ecdysis behavior of the red flour beetle, *Tribolium castaneum*. *Mech. Dev.* **125**, 984-995.

Babcock, D. T., Brock, A. R., Fish, G. S., Wang, Y., Perrin, L., Krasnow, M. A. and Galko, M. J. (2008). Circulating blood cells function as a surveillance system for damaged tissue in *Drosophila* larvae. *Proc. Natl. Acad. Sci. USA* **105**, 10017-10022.

Belmont, M., Cazzamali, G., Williamson, M., Hauser, F. and Grimmelikhuijzen, C. J. P. (2006). Identification of four evolutionarily related G protein-coupled receptors from the malaria mosquito Anopheles gambiae. *Biochem. Biophys. Res. Commun.* **344**, 160-165.

Boerjan, B., Verleyen, P., Huybrechts, J., Schoofs, L. and De Loof, A. (2010). In search for a common denominator for the diverse functions of arthropod corazonin: a role in the physiology of stress? *Gen. Comp. Endocrinol.* **166**, 222-233.

Cheung, C. C., Loi, P. K., Sylwester, A. W., Lee, T. D. and Tublitz, N. J. (1992). Primary structure of a cardioactive neuropeptide from the tobacco hawkmoth, *Manduca sexta*. *FEBS Lett.* **313**, 165-168.

Christie, A. E., Nolan, D. H., Ohno, P., Hartline, N. and Lenz, P. H. (2011). Identification of chelicerate neuropeptides using bioinformatics of publicly accessible expressed sequence tags. *Gen. Comp. Endocrinol.* **170**, 144-155.

Chung, J. S., Wilcockson, D. C., Zmora, N., Zohar, Y., Dircksen, H. and Webster, S. G. (2006). Identification and developmental expression of mRNAs encoding crustacean cardioactive peptide (CCAP) in decapod crustaceans. *J. Exp. Biol.* **209**, 3862-3872.

Coggins, S. A., Estévez-Lao, T. Y. and Hillyer, J. F. (2012). Increased survivorship following bacterial infection by the mosquito Aedes aegypti as compared to *Anopheles gambiae* correlates with increased transcriptional induction of antimicrobial peptides. *Dev. Comp. Immunol.* **37**, 390-401.

da Silva, S. R., da Silva, R. and Lange, A. B. (2011). Effects of crustacean cardioactive peptide on the hearts of two Orthopteran insects, and the demonstration of a Frank-Starling-like effect. *Gen. Comp. Endocrinol.* **171**, 218-224.

Davis, N. T., Dulcis, D. and Hildebrand, J. G. (2001). Innervation of the heart and aorta of *Manduca sexta*. *J. Comp. Neurol.* **440**, 245-260.

Dircksen, H., Neupert, S., Predel, R., Verleyen, P., Huybrechts, J., Strauss, J., Hauser, F., Stafflinger, E., Schneider, M., Pauwels, K. et al. (2011). Genomics, transcriptomics, and peptidomics of *Daphnia pulex* neuropeptides and protein hormones. *J. Proteome Res.* **10**, 4478-4504.

Donini, A., Agricola, H. and Lange, A. B. (2001). Crustacean cardioactive peptide is a modulator of oviduct contractions in *Locusta migratoria*. *J. Insect Physiol.* **47**, 277-285.

Dulcis, D. and Levine, R. B. (2003). Innervation of the heart of the adult fruit fly, *Drosophila melanogaster*. *J. Comp. Neurol.* **465**, 560-578.

Dulcis, D. and Levine, R. B. (2005). Glutamatergic innervation of the heart initiates retrograde contractions in adult *Drosophila melanogaster*. *J. Neurosci.* **25**, 271-280.

Dulcis, D., Davis, N. T. and Hildebrand, J. G. (2001). Neuronal control of heart reversal in the hawkmoth *Manduca sexta*. *J. Comp. Physiol. A* **187**, 837-849.

Dulcis, D., Levine, R. B. and Ewer, J. (2005). Role of the neuropeptide CCAP in *Drosophila* cardiac function. *J. Neurobiol.* **64**, 259-274.

Ejaz, A. and Lange, A. B. (2008). Peptidergic control of the heart of the stick insect, *Baculum extradentatum*. *Peptides* **29**, 214-225.

Ewer, J. and Reynolds, S. (2002). Neuropeptide control of molting in insects. In *Hormones, Brain and Behavior*, Vol. 3 (ed. D. W. Pfaff, A. P. Arnold, A. M. Etgen, S. E. Fahrbach and R. T. Rubin), pp. 1-92. San Diego, CA: Academic Press.

Ewer, J., Wang, C. M., Klukas, K. A., Mesce, K. A., Truman, J. W. and Fahrbach, S. E. (1998). Programmed cell death of identified peptidergic neurons involved in ecdysis behavior in the moth, *Manduca sexta*. *J. Neurobiol.* **37**, 265-280.

Furuya, K., Liao, S., Reynolds, S. E., Ota, R. B., Hackett, M. and Schooley, D. A. (1993). Isolation and identification of a cardioactive peptide from *Tenebrio molitor* and *Spodoptera eridania*. *Biol. Chem. Hoppe Seyler* **374**, 1065-1074.

Glenn, J. D., King, J. G. and Hillyer, J. F. (2010). Structural mechanics of the mosquito heart and its function in bidirectional hemolymph transport. *J. Exp. Biol.* **213**, 541-550.

Hillyer, J. F., Barreau, C. and Vernick, K. D. (2007). Efficiency of salivary gland invasion by malaria sporozoites is controlled by rapid sporozoite destruction in the mosquito haemocoel. *Int. J. Parasitol.* **37**, 673-681.

Hillyer, J. F., Estévez-Lao, T. Y., Funkhouser, L. J. and Aluoch, V. A. (2012). *Anopheles gambiae* corazonin: gene structure, expression and effect on mosquito heart physiology. *Insect Mol. Biol.* **21**, 343-355.

Honegger, H.-W., Dewey, E. M. and Ewer, J. (2008). Bursicon, the tanning hormone of insects: recent advances following the discovery of its molecular identity. *J. Comp. Physiol. A* **194**, 989-1005.

Honegger, H.-W., Estévez-Lao, T. Y. and Hillyer, J. F. (2011). Bursicon-expressing neurons undergo apoptosis after adult ecdysis in the mosquito *Anopheles gambiae*. *J. Insect Physiol.* **57**, 1017-1022.

Johnson, E., Ringo, J. and Dowse, H. (1997). Modulation of *Drosophila* heartbeat by neurotransmitters. *J. Comp. Physiol. B* **167**, 89-97.

Jones, J. C. (1977). *The Circulatory System of Insects*. Springfield, IL: Charles C. Thomas.

Klowden, M. J. (2007). Circulatory systems. In *Physiological Systems in Insects*, 2nd edn, pp. 357-401. Boston, MA: Academic Press.

Kostron, B., Kaltenhauser, U., Seibel, B., Bräunig, P. and Honegger, H. (1996). Localization of bursicon in CCAP-immunoreactive cells in the thoracic ganglia of the cricket *Gryllus bimaculatus*. *J. Exp. Biol.* **199**, 367-377.
Lahr, E. C., Dean, D. and Ewer, J. (2012). Genetic analysis of ecdysis behavior in *Drosophila* reveals partially overlapping functions of two unrelated neuropeptides. *J. Neurosci.* **32**, 6819-6829.
Lee, H. and Lange, A. B. (2011). Crustacean cardioactive peptide in the Chagas' disease vector, *Rhodnius prolixus*: presence, distribution and physiological effects. *Gen. Comp. Endocrinol.* **174**, 36-43.
Lee, D. H., Paluzzi, J. P., Orchard, I. and Lange, A. B. (2011). Isolation, cloning and expression of the crustacean cardioactive peptide gene in the Chagas' disease vector, *Rhodnius prolixus*. *Peptides* **32**, 475-482.
Lee, D., Taufique, H., da Silva, R. and Lange, A. B. (2012). An unusual myosuppressin from the blood-feeding bug *Rhodnius prolixus*. *J. Exp. Biol.* **215**, 2088-2095.
Lehman, H. K., Murgiuc, C. M., Miller, T. A., Lee, T. D. and Hildebrand, J. G. (1993). Crustacean cardioactive peptide in the sphinx moth, *Manduca sexta*. *Peptides* **14**, 735-741.
Li, B., Beeman, R. W. and Park, Y. (2011). Functions of duplicated genes encoding CCAP receptors in the red flour beetle, *Tribolium castaneum*. *J. Insect Physiol.* **57**, 1190-1197.
Livak, K. J. and Schmittgen, T. D. (2001). Analysis of relative gene expression data using real-time quantitative PCR and the $2^{-\Delta\Delta C_T}$ method. *Methods* **25**, 402-408.
Loi, P. K., Emmal, S. A., Park, Y. and Tublitz, N. J. (2001). Identification, sequence and expression of a crustacean cardioactive peptide (CCAP) gene in the moth *Manduca sexta*. *J. Exp. Biol.* **204**, 2803-2816.
Nation, J. L. (2008). Circulatory system. In *Insect Physiology and Biochemistry*, pp. 339-365. Boca Raton, FL: CRC Press.
Nichols, R. (2006). FMRFamide-related peptides and serotonin regulate *Drosophila melanogaster* heart rate: mechanisms and structure requirements. *Peptides* **27**, 1130-1137.
Nichols, R., Kaminski, S., Walling, E. and Zornik, E. (1999). Regulating the activity of a cardioacceleratory peptide. *Peptides* **20**, 1153-1158.
Park, J. H., Schroeder, A. J., Helfrich-Förster, C., Jackson, F. R. and Ewer, J. (2003). Targeted ablation of CCAP neuropeptide-containing neurons of *Drosophila* causes specific defects in execution and circadian timing of ecdysis behavior. *Development* **130**, 2645-2656.
Petersen, T. N., Brunak, S., von Heijne, G. and Nielsen, H. (2011). SignalP 4.0: discriminating signal peptides from transmembrane regions. *Nat. Methods* **8**, 785-786.
Predel, R., Neupert, S., Garczynski, S. F., Crim, J. W., Brown, M. R., Russell, W. K., Kahnt, J., Russell, D. H. and Nachman, R. J. (2010). Neuropeptidomics of the mosquito *Aedes aegypti*. *J. Proteome Res.* **9**, 2006-2015.
Riehle, M. A., Garczynski, S. F., Crim, J. W., Hill, C. A. and Brown, M. R. (2002). Neuropeptides and peptide hormones in Anopheles gambiae. *Science* **298**, 172-175.
Sakai, T., Satake, H., Minakata, H. and Takeda, M. (2004). Characterization of crustacean cardioactive peptide as a novel insect midgut factor: isolation, localization, and stimulation of alpha-amylase activity and gut contraction. *Endocrinology* **145**, 5671-5678.
Setzu, M., Biolchini, M., Lilliu, A., Manca, M., Muroni, P., Poddighe, S., Bass, C., Angioy, A. M. and Nichols, R. (2012). Neuropeptide F peptides act through unique signaling pathways to affect cardiac activity. *Peptides* **33**, 230-239.
Simo, L., Slovák, M., Park, Y. and Zitnan, D. (2009). Identification of a complex peptidergic neuroendocrine network in the hard tick, *Rhipicephalus appendiculatus*. *Cell Tissue Res.* **335**, 639-655.
Sláma, K. and Lukáš, J. (2011). Myogenic nature of insect heartbeat and intestinal peristalsis, revealed by neuromuscular paralysis caused by the sting of a braconid wasp. *J. Insect Physiol.* **57**, 251-259.
Stangier, J., Hilbich, C., Beyreuther, K. and Keller, R. (1987). Unusual cardioactive peptide (CCAP) from pericardial organs of the shore crab *Carcinus maenas*. *Proc. Natl. Acad. Sci. USA* **84**, 575-579.
Tawfik, A. I., Tanaka, S., De Loof, A., Schoofs, L., Baggerman, G., Waelkens, E., Derua, R., Milner, Y., Yerushalmi, Y. and Pener, M. P. (1999). Identification of the gregarization-associated dark-pigmentotropin in locusts through an albino mutant. *Proc. Natl. Acad. Sci. USA* **96**, 7083-7087.
Veelaert, D., Passier, P., Devreese, B., Vanden Broeck, J., Van Beeumen, J., Vullings, H. G., Diederen, J. H., Schoofs, L. and De Loof, A. (1997). Isolation and characterization of an adipokinetic hormone release-inducing factor in locusts: the crustacean cardioactive peptide. *Endocrinology* **138**, 138-142.
Veenstra, J. A. (2000). Mono- and dibasic proteolytic cleavage sites in insect neuroendocrine peptide precursors. *Arch. Insect Biochem. Physiol.* **43**, 49-63.
Veenstra, J. A. (2009). Does corazonin signal nutritional stress in insects? *Insect Biochem. Mol. Biol.* **39**, 755-762.
Wasielewski, O. and Skonieczna, M. (2008). Pleiotropic effects of the neuropeptides CCAP and myosuppressin in the beetle, *Tenebrio molitor* L. *J. Comp. Physiol. B* **178**, 877-885.
Wasserthal, L. (2003). Circulation and thermoregulation. In *Lepidoptera, Moths and Butterflies: Morphology, Physiology, and Development*, Vol. 2 (ed. N. Kristensen), pp. 205-228. New York, NY: Walter De Gruyter.
Wasserthal, L. T. (2007). Drosophila flies combine periodic heartbeat reversal with a circulation in the anterior body mediated by a newly discovered anterior pair of ostial valves and 'venous' channels. *J. Exp. Biol.* **210**, 3707-3719.
Wasserthal, L. T. (2012). Influence of periodic heartbeat reversal and abdominal movements on hemocoelic and tracheal pressure in resting blowflies *Calliphora vicina*. *J. Exp. Biol.* **215**, 362-373.
Woodruff, E. A., 3rd, Broadie, K. and Honegger, H.-W. (2008). Two peptide transmitters co-packaged in a single neurosecretory vesicle. *Peptides* **29**, 2276-2280.